Temperature-programmed desorption of H_2 from molybdenum nitride thin films

Jeong-Gil Choi, Hyuek Joon Lee, Levi T. Thompson *

Department of Chemical Engineering, The University of Michigan, Ann Arbor, MI 48109, USA

Abstract

The thermal desorption of hydrogen from β-$Mo_{16}N_7$, γ-Mo_2N and δ-MoN thin films was investigated. Hydrogen adsorption at ~ 270 K produced two hydrogen desorption peaks, one at ~ 370 K (designated as the β_1 site) and the other at ~ 800 K (designated as the β_2 site). We concluded that the β_1 peak was due to a low-energy surface site and the β_2 peak to a subsurface site. Desorption from the β_1 state obeyed first-order kinetics. The hydrogen saturation capacity increased in the following order: β-$Mo_{16}N_7$ < δ-MoN < γ-Mo_2N. This variation in saturation coverage tracked with the nominal molybdenum atom surface density. Nitrogen also desorbed from the Mo nitride surfaces during the H_2 temperature-programmed desorption experiments producing a low-temperature peak at ~ 370 K and several high-temperature peaks in the range 500–900 K. The amount of nitrogen that desorbed increased with increasing H_2 dose, suggesting a hydrogen-induced nitrogen desorption process. Hydrogen may have weakened the Mo–N bond thereby facilitating the desorption of nitrogen. We believe that the low-temperature peak was due to nitrogen bound to Mo atoms at the surface. The high-temperature peaks were probably a consequence of hydrogen that diffused into the surface altering the Mo–N bonding in the subsurface region. Thermal desorption characteristics of the Mo nitride films were similar to those of a series of bulk γ-Mo_2N powders that we previously investigated. Apparent energies for hydrogen desorption from the low-temperature sites were near 25 kcal/mol, and both the thin films and powders possessed high-temperature subsurface binding sites. The most striking observation was the similarity between the characters of the δ-MoN film and the Mo nitride powder with the highest hydrodenitrogenation activity. This similarity suggested that the high activity was due to the presence of δ-MoN-like structures at or near the bulk powder surface.

1. Introduction

Since the report by Volpe and Boudart that early transition-metal nitrides and carbides can be prepared in high-surface-area form [1,2], nitrides and carbides have received a great deal of attention. They are competitively active for reactions including ammonia synthesis [3], hydrodenitrogenation [4] and CO hydrogenation [5]. In addition, early transition-metal carbides possess catalytic properties that are similar to those of noble metals like Pt [6]. Despite the interest in these

* Corresponding author. Tel.: (313) 936-2015; Fax: (313) 763-0459.

materials, there is very little known about the influence of surface structure and composition on their catalytic properties.

The focus of our research has been on the Mo nitride system [7,8]. Three equilibrium Mo nitride phases are known: β-Mo$_{16}$N$_7$ (body-centered tetragonal), γ-Mo$_2$N (face-centered cubic), and δ-MoN (hexagonal) [phase diagram]. Most high-surface-area Mo nitrides contain only γ-Mo$_2$N in the bulk [3–5]. We recently found that the surface and bulk properties of a series of high-surface-area γ-Mo$_2$N powders were very different [7,9]. The near-surface molybdenum to nitrogen atomic ratios for most of the powders were near unity, the value expected for δ-MoN. Structures near the surface were body-centered like β-Mo$_{16}$N$_7$. As has been done with metal catalysts, we believe that model molybdenum nitride surfaces can be used to better understand the catalytic properties of high-surface-area molybdenum nitrides. Recently, Bafrali and Bell [10] reported the results of a H$_2$ temperature-programmed desorption study of Mo(100)-c(2 × 2)N. They suggested that the c(2 × 2) array of nitrogen atoms on the Mo(100) surface produced a structure nearly identical to the γ-Mo$_2$N(200) surface.

The purpose of the research described in this paper was to evaluate the surface chemical properties of well-defined β-Mo$_{16}$N$_7$, γ-Mo$_2$N and δ-MoN films. The films were prepared by codepositing Mo atoms and nitrogen ions [11]. Here we present the H$_2$ temperature-programmed desorption (TPD) results. These results were compared to those for clean and nitrided Mo single crystals, and bulk Mo nitride powders.

2. Experimental details

Preferentially oriented β-Mo$_{16}$N$_7$, γ-Mo$_2$N and δ-MoN films were synthesized using Ion Beam Assisted Deposition (IBAD). Ion Beam Assisted Deposition involves the simultaneous deposition of atoms and low-energy ions. The molybdenum was deposited at a rate of 5 to 6 Å/s onto single-crystal Si(100) substrates using an electron beam evaporator. The nitrogen ion flux was adjusted to achieve the desired film

properties. Depositions were carried out using 500 eV nitrogen ions with a nitrogen-backfill pressure of 5×10^{-5} Torr inside the deposition chamber. The ion flux was measured using three Faraday cups placed around the sample in a circular fashion. Additional details concerning the deposition of these films, and their compositions and structures can be found elsewhere [11]. Properties of the Mo nitride thin films are summarized in Table 1. The nominal surface Mo densities were determined based on the preferentially oriented planes identified from X-ray diffraction analysis. The surface compositions were determined using X-ray photoelectron spectroscopy (VSW Class 150 hemispherical analyzer with a TA10 X-ray source). Typically the Mg Kα line was used. Gaussian and/or Lorentzian peaks were deconvoluted using a non-linear least-squares algorithm [7]. The atomic compositions were estimated based on comparisons of the integrated peak intensities normalized by the atomic sensitivity factors. The atomic sensitivity factors for the Mo(3d$_{5/2}$), Mo(3p$_{3/2}$), and N(1s) peaks were 1.66, 1.17, and 0.42, respectively [12]. Uncertainties in the composition were expected to be ~ 15%.

The thermal desorption experiments were performed in an ultra-high vacuum chamber. After bake-out, the base pressure in the chamber was less than 8×10^{-10} Torr. The sample was mounted onto a Mo platen and heated by radiation from a tungsten filament located 5 mm behind the platen. A heating rate of ~ 6 K/s was used for most of the experiments except for sev-

Table 1
Properties of the Mo nitride thin films

Film	Crystal structure and orientation	Nominal Mo surface site density (Mo/cm^2)	N/Mo ratio [a]	
			RBS	XPS
β-Mo$_{16}$N$_7$	bct (400)	0.15×10^{15}	0.72	0.44
γ-Mo$_2$N	fcc (200)	1.14×10^{15}	0.35	0.46
δ-MoN	hex (101)	0.22×10^{15}	1.18	0.62

[a] The N/Mo ratios are averages from Rutherford backscattering spectrometry (RBS) and X-ray photoelectron spectroscopy (XPS).

eral experiments which were performed to investigate the effect of heating rate. The samples were heated to 950 K during the TPD experiments. Sample cooling was achieved by conduction through a copper block in thermal contact with a liquid-nitrogen reservoir. Hydrogen was introduced directly to the film face through a stainless-steel variable leak valve. The distance between the end of the doser and the sample was approximately 5 mm. The sample was turned to face the mass spectrometer during the TPD experiments to enhance the signal-to-noise ratio and minimize the effect of differing pumping speeds on the detection sensitivity for the various products. During routine TPD experiments H_2 was adsorbed at ~ 270 K, and the desorption of H_2, NH_3, H_2O, N_2 and CO_2 or N_2O was monitored by measuring the signals for $m/e = 2, 17, 18, 28$ and 44, respectively. All data reported here were obtained by collecting intensity–temperature profiles for five masses in a given experiment. Another program allowed collection of up to 100 masses in a given experiment [13] and was used to check for unanticipated products. The sample surface was cleaned by sputtering with 500 eV Ar^+ ions at ambient temperature. Occasionally the samples were sputtered between runs using a VSW AS10 ion source to expose a fresh surface. A sputter time of 5 min corresponded to the removal of ~ 10 Å. Annealing the films prior to the TPD experiment did not significantly alter the TPD or XPS spectra suggesting that there was no significant reconstruction.

3. Results

3.1. β-$Mo_{16}N_7$ thin film

Fig. 1 shows the H_2 TPD spectra for the β-$Mo_{16}N_7$ film as a function of dose given in units of langmuir (10^6 Torr · s). The curves corresponding to different doses have been displaced vertically for clarity in this and other spectra. There were two predominant peaks: a low-temperature peak centered at ~ 370 K (designated as the β_1 site) and a high-temperature peak centered at ~ 800 K (designated as the β_2 site). The

high-temperature site was populated before the low-temperature site was populated.

The β_1 peak did not shift with increasing dose, indicating a first-order desorption process [14,15]. One can determine apparent desorption energies from the TPD spectra. For first-order desorption with $10^8 < \nu_0/\alpha < 10^{13}$ K^{-1}, the desorption energy is given to within 1.5% by [16]

$$E = RT_p\left[\ln(\nu_0 T_p/\alpha) - 3.64\right], \tag{1}$$

where ν_0 is the pre-exponential factor, α is the heating rate, R is the gas constant, and T_p is the absolute temperature for the maximum desorption rate. The desorption energy can be estimated directly from the measured T_p. We could not independently determine the pre-exponential factor, so a value was assumed. A pre-exponential factor of 10^{13} s^{-1} is often used [16–18]. Typically, desorption energies are not very sensitive to even order of magnitude changes in ν_0. Assuming a pre-exponential factor of 10^{13} s^{-1}, the apparent desorption energy for the β_1 site was 22 kcal/mol. This is similar to the estimate of 21 kcal/mol for hydrogen desorption from Mo(100) [18] although the process was reported to be second order. It was difficult to determine whether the β_2 state followed first- or second-order kinetics, although the fairly constant peak temperature with increasing dose suggested first-order kinetics in the mid-
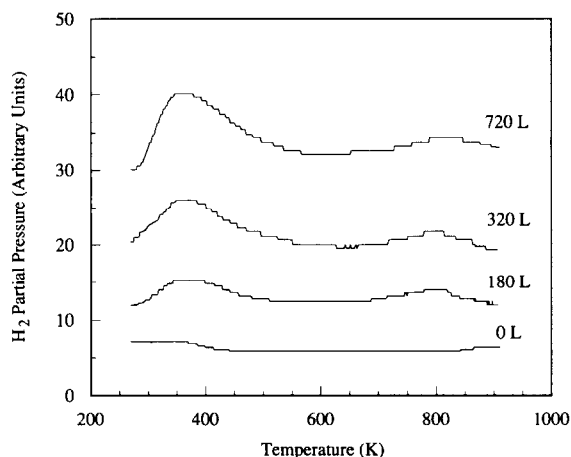

Fig. 1. Hydrogen temperature-programmed desorption from the β-$Mo_{16}N_7$ film as a function of dose (given in units of langmuir or 10^6 Torr·s).

dle range of dose. If we assume that desorption from the β_2 site was first order with $\nu_0 = 10^{13}$ s^{-1}, the desorption energy was calculated to be 50 kcal/mol.

During the H_2 TPD experiments, N_2 also desorbed from the β-Mo$_{16}$N$_7$ surface (Fig. 2). No species other than H_2 and N_2 were detected (Fig. 3). The N_2 desorption spectrum consisted of a low-temperature peak centered at ~ 350 K and several high-temperature peaks in a broad range between 500 and 900 K. Nitrogen at or near the film surface was the only source of N_2. The amount of N_2 that desorbed increased with increasing H_2 dose. This result indicated that there was a relationship between the amount of hydrogen adsorbed and the nitrogen that desorbed.

3.2. γ-Mo$_2$N thin film

Fig. 4 shows the H_2 TPD spectra for the γ-Mo$_2$N film. As the H_2 dose was increased, the maximum rate of desorption increased and the peaks sharpened. The hydrogen desorption peaks were centered at ~ 375 and ~ 850 K. Positions of the H_2 peaks for the γ-Mo$_2$N film were very close to those for the β-Mo$_{16}$N$_7$ film, however, the maximum desorption rates were much higher. Since the dimensions of the films were similar, this result indicated that the γ-Mo$_2$N surface had a greater H_2 saturation capacity than did the β-Mo$_{16}$N$_7$ surface. As the γ-Mo$_2$N(200) surface
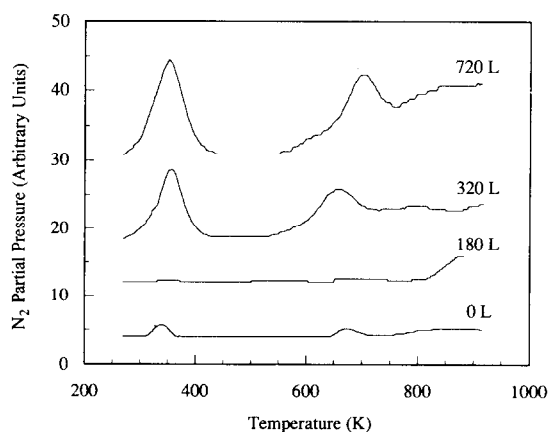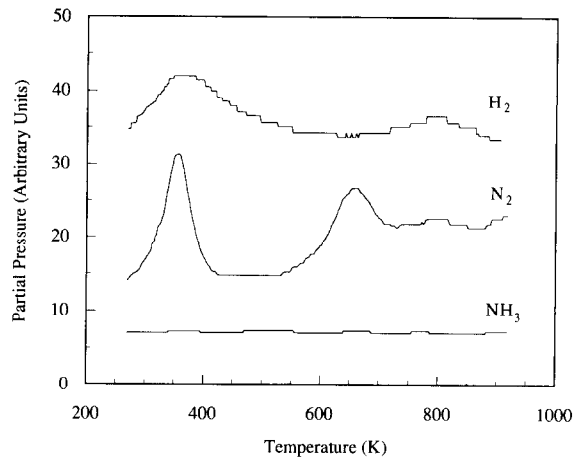
Fig. 3. Desorption of H_2, N_2 and NH_3 following a H_2 dose of 320 L to the surface of the β-Mo$_{16}$N$_7$ film.

has a higher Mo site density than the β-Mo$_{16}$N$_7$(400) surface (see Table 1), this result seemed reasonable. It is also possible that the difference in adsorption capacity was due to the different surface structures. β-Mo$_{16}$N$_7$ is body-centered tetragonal while γ-Mo$_2$N is face-centered cubic, consequently molybdenum atoms on a β-Mo$_{16}$N$_7$(400) surface have different symmetries than those on a γ-Mo$_2$N(200) surface. Structure dependence for the desorption of hydrogen is supported by our observation that the near-surface N/Mo stoichiometries for
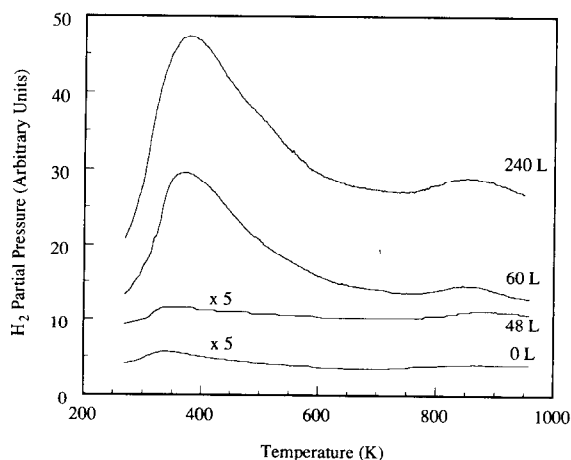

Fig. 2. Desorption of N_2 following various H_2 doses to the surface of the β-Mo$_{16}$N$_7$ film.

Fig. 4. Hydrogen temperature-programmed desorption from the γ-Mo$_2$N film as a function of dose.

the γ-Mo$_2$N and β-Mo$_{16}$N$_7$ films were similar (Table 1).

Desorption energies for the β_1 and β_2 states on γ-Mo$_2$N were determined using the Redhead equation [16]. Given the fairly constant peak temperatures with increasing dose, first-order desorption was assumed. Using a pre-exponential factor of 10^{13} s^{-1}, the desorption energies for the β_1 and β_2 states were estimated to be 23 and 53 kcal/mol, respectively. These values were close to those determined for the β-Mo$_{16}$N$_7$ film.

The low-temperature H$_2$ TPD character for the γ-Mo$_2$N film was similar to that reported for Mo(100)-c(2 × 2)N, the proposed analog of the γ-Mo$_2$N(200) surface, but their high-temperature characters were very different. Hydrogen desorption from Mo(100)-c(2 × 2)N produced TPD peaks at ~ 350 and 500 K for a heating rate of 21 K/s [10]. The peak temperature for the low-temperature state was constant with dose suggesting first-order desorption. We calculated an apparent desorption energy of ~ 20 kcal/mol for this low-temperature site, assuming first-order kinetics and a pre-exponential factor of 10^{13} s^{-1}.

As we found for the β-Mo$_{16}$N$_7$ film, N$_2$ desorbed from the γ-Mo$_2$N film during the H$_2$ TPD experiments (Fig. 5). While the positions for the low-temperature peaks were similar, there were subtle differences between the high-temperature
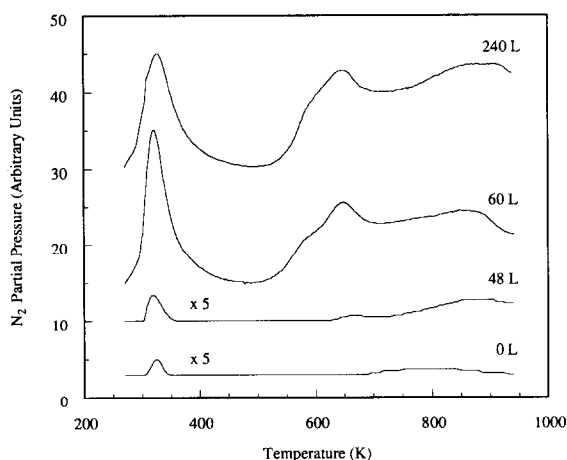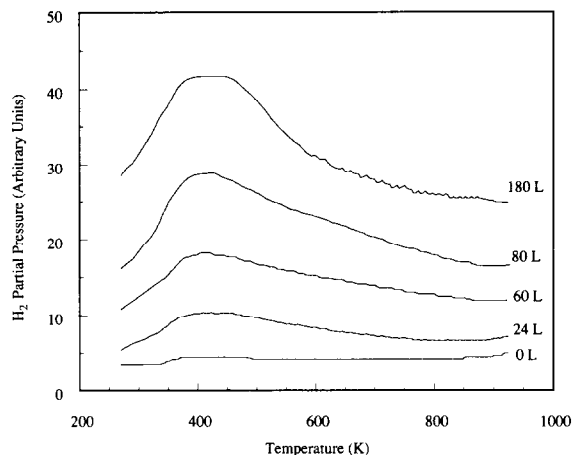

Fig. 6. Hydrogen temperature-programmed desorption from the δ-MoN film as a function of dose.

desorption peaks for the γ-Mo$_2$N and β-Mo$_{16}$N$_7$ films.

3.3. δ-MoN thin film

Fig. 6 shows the H$_2$ TPD spectra for the δ-MoN film. The maximum desorption rate increased with increasing hydrogen dose. Unlike the γ-Mo$_2$N and β-Mo$_{16}$N$_7$ films, only one peak was observed within the temperature and dose range studied. This peak appeared at ~ 420 K and was much broader than peaks for the other two films. Furthermore, the H$_2$ desorption peak for the δ-MoN film was asymmetric. It was clear that the surface characteristics of the δ-MoN film were significantly different from those of the β-Mo$_{16}$N$_7$ and γ-Mo$_2$N films. First-order desorption was assumed for the δ-MoN film since the peak temperature did not shift with dose. The desorption energy was estimated to be 26 kcal/mol which is slightly higher than those determined for the β-Mo$_{16}$N$_7$ and γ-Mo$_2$N films.

Nitrogen also desorbed from the δ-MoN film during each H$_2$ TPD experiment. Fig. 7 compares the N$_2$ desorption spectra for the β-Mo$_{16}$N$_7$, γ-Mo$_2$N and δ-MoN films. Each showed a sharp low-temperature peak but there were slight differences between their behaviors at high temperature. A more significant difference was observed
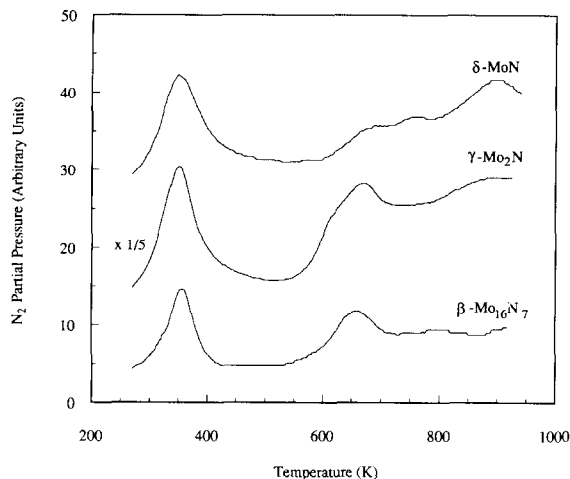

Fig. 5. Desorption of N$_2$ following various H$_2$ doses to the surface of the γ-Mo$_2$N film.

Fig. 7. Comparison of the N_2 desorption spectra for the β-$Mo_{16}N_7$, γ-Mo_2N and δ-MoN films.

between the amount of nitrogen desorbed at low temperature. The nitrogen desorption rate from the δ-MoN film was intermediate to those from the β-$Mo_{16}N_7$ and γ-Mo_2N films and tracked to some extent with variations in the Mo surface atom densities.

4. Discussion

4.1. H_2 TPD from Mo nitride thin films

While there were significant differences between the H_2 TPD spectra for the β-$Mo_{16}N_7$, γ-Mo_2N and δ-MoN films, there were also several strong similarities. A low-temperature peak due to a first-order event was observed for each of the films. The position of this peak was approximately the same for the β-$Mo_{16}N_7$ and γ-Mo_2N films. A second peak was also observed at higher temperatures for the β-$Mo_{16}N_7$ and γ-Mo_2N.

The results for the Mo nitride films were different from those reported for Mo [18,19] and Mo(100)-c(2 × 2)N single crystals [10]. While hydrogen adsorption produced low-temperature desorption peaks with maxima in similar ranges for the Mo nitride films, Mo(100) and Mo(100)-c(2 × 2)N, the high-temperature characteristics

were very different. We concluded that desorption from the low- and high-temperature states for the Mo nitride films was first order. Han and Schmidt [19] indicated that on Mo(100) the low-temperature state obeyed first-order kinetics, but the two higher temperature states followed second-order desorption kinetics. Zaera et al. [18] reported the presence of three different sites on Mo(100) but concluded that hydrogen desorption from all three was second order. More recently, Bafrali and Bell [10] identified three peaks during H_2 TPD from Mo(100) and two peaks from Mo(100)-c(2 × 2)N. Variations in the TPD spectra for Mo(100)-c(2 × 2)N with dose were consistent with the low-temperature state being first order and the high-temperature state being second order.

Previously we reported that hydrogen populated subsurface sites in bulk Mo nitride powders [7]. In order to probe for the presence of subsurface hydrogen binding sites in the Mo nitride films, TPD experiments were performed using different heating rates. Experimentally, desorption peaks produced by surface sites can be distinguished from those produced by subsurface sites by examining the effect of heating rate on the TPD spectrum. Variations in the heating rate should not influence the relative sizes of peaks due to surface sites. A change in the relative intensities with varying heating rate reflects the presence of subsurface sites [20]. We found that the relative intensities of peaks in the TPD spectra changed dramatically with the heating rate (Figs. 8 and 9). This result suggested that the β_2 peak was produced by desorption from subsurface sites. Conceptually, this can be understood as hydrogen penetrating into the subsurface, diffusing back to the surface during subsequent heating, then desorbing to produce a high-temperature peak. The presence of subsurface hydrogen was supported by two other observations. After each TPD experiment the film was annealed to ensure that the surface was clean. In almost every case H_2, in amounts in excess of monolayer coverage, was removed from the film. This result suggested the presence of a subsurface or bulk hydrogen reservoir. After carrying out a standard H_2 TPD experiment, the sample
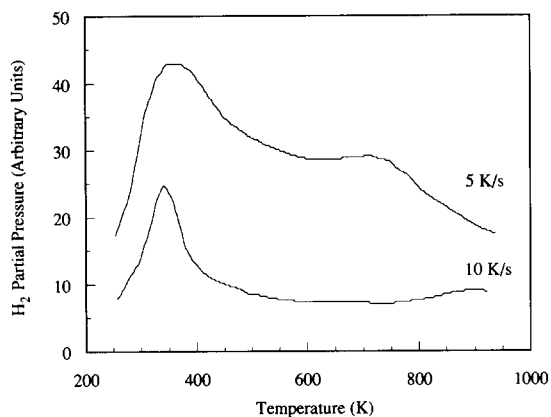
Fig. 8. Hydrogen temperature-programmed desorption from the β-Mo$_{16}$N$_7$ film at different heating rates. The hydrogen dose was 420 L.

Fig. 10. Typical hydrogen temperature-programmed desorption spectra for the (a) low-, (b) medium- and (c) high-surface-area molybdenum nitride powders [7].

was cooled to ~ 270 K, then sputtered for 5 min. Immediately after sputtering, the sample was heated linearly without further exposure to hydrogen. The resulting TPD spectrum was similar to that collected during a normal experiment. As the H$_2$ pressure in the chamber and time between sputtering and heating were low, we can rule out readsorption as the source of this behavior. A speculative explanation is that after sputtering, which removed ~ 10 Å from the surface, hydrogen previously in the subsurface was exposed.

Our observation that the intensity of the high-temperature peak leveled off with increasing hy-
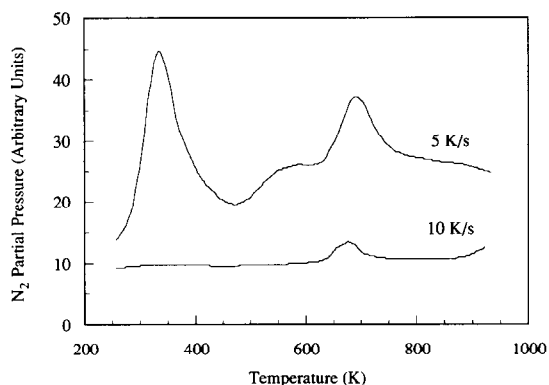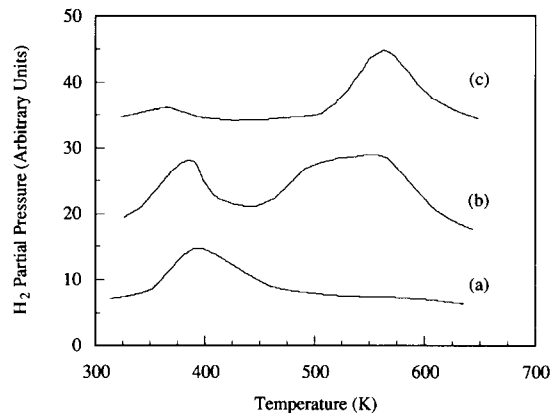
drogen dose suggested that the subsurface hydrogen reservoir was of limited extent. We believe that the subsurface layer separates the free surface from the bulk and is only a few atomic layers thick. While surface, subsurface and bulk sites can be populated during exposure to hydrogen, it is possible that only hydrogen at the surface or in the subsurface layer is removed during TPD. This scenario would account for our observations and the saturation of subsurface hydrogen sites.

4.2. Comparison of Mo nitride thin films and powders

Hydrogen desorption from the Mo nitride thin films was compared with that from a series of bulk Mo nitride powders with surface areas ranging up to 120 m^2/g. The TPD experiments for the Mo nitride powders were conducted following saturation of the surface with H$_2$ at ~ 300 K [8]. In general, there were three peaks observed using a heating rate of 0.25 K/s. Fig. 10 shows typical H$_2$ TPD spectra for the low-, medium- and high-surface-area nitrides. Incidentally, the lowest-surface-area material possessed the highest activity for pyridine hydrodenitrogenation, while the highest-surface-area material was the least active. The two low-temperature peaks were due to surface sites while the high-temperature peak was attributed to a subsurface site [7]. The lowest-

Fig. 9. Desorption of N$_2$ from the β-Mo$_{16}$N$_7$ film during H$_2$ temperature-programmed desorption at different heating rates. The hydrogen dose was 420 L.

temperature peaks for the Mo nitride powders were in a similar range as those for the thin films. Desorption from surface sites on the thin films and powders appeared to be first order with apparent energies of ~ 22 kcal/mol. Desorption from subsurface sites in the thin films appeared to be first order with an apparent energy of ~ 50 kcal/mol, while that from the powders was second order with an apparent desorption energy of ~ 12 kcal/mol. The relatively low apparent energy for desorption from the powders may have been a consequence of facilitated diffusion. Diffusion is facile along grain boundaries, interfaces and dislocations compared to diffusion through the crystal [21].

There was a striking similarity between the qualitative character of the δ-MoN film and the lowest surface area, highest activity Mo nitride powder. While the lower activity catalysts produced two desorption peaks, the most active material produced only one low-temperature peak. This peak was asymmetric as was the peak for the δ-MoN film. The H_2 desorption energy for the highest activity powder was 24 kcal/mol compared to 26 kcal/mol for the δ-MoN film. While the primary bulk phase in the powder was γ-Mo_2N as determined by X-ray diffraction, the near-surface N/Mo stoichiometry was consistent with the presence of MoN [9]. This may have been the reason why the desorption properties for the high activity powder were similar to those of the δ-MoN film.

4.3. Hydrogen-induced nitrogen desorption

Nitrogen desorption was observed during hydrogen desorption from the Mo nitride thin films. Variations in the nitrogen content at or near the surface as determined using XPS were somewhat consistent with the loss of small amounts of nitrogen from the film. In most cases the N/Mo atomic ratio decreased slightly following TPD (Fig. 11). A large nitrogen desorption peak was observed at ~ 330 K for all the samples during H_2 TPD. Given the low temperature, we concluded that this peak was due to nitrogen weakly bound to molybdenum surface atoms. Character-

istics of the higher-temperature peaks were complex and different for each sample.

The maximum rates for nitrogen desorption increased with increasing H_2 dose suggesting that the nitrogen desorption was induced by the presence of hydrogen. The desorption of nitrogen in the absence of H_2 typically did not occur to any significant extent at temperatures less than 1000 K. Hydrogen adsorbed at the surface may have weakened the bonding between nitrogen and Mo thus causing nitrogen to desorb at a relatively low temperature. We suspect that the high-temperature nitrogen desorption peaks observed for the thin films were caused by hydrogen that diffused into the subsurface layer. This hydrogen may also have weakened the Mo–N bonds facilitating the diffusion of nitrogen out of the subsurface region to the surface during heating.

5. Conclusion

The temperature-programmed desorption of H_2 from β-$Mo_{16}N_7$, γ-Mo_2N and δ-MoN films was studied. There were two types of hydrogen desorption sites: a low-energy site producing a peak at ~ 370 K (designated as β_1) and a high-energy site giving rise to a peak at ~ 800 K (designated as β_2). Each of the films possessed β_1 sites but only the β-$Mo_{16}N_7$ and γ-Mo_2N
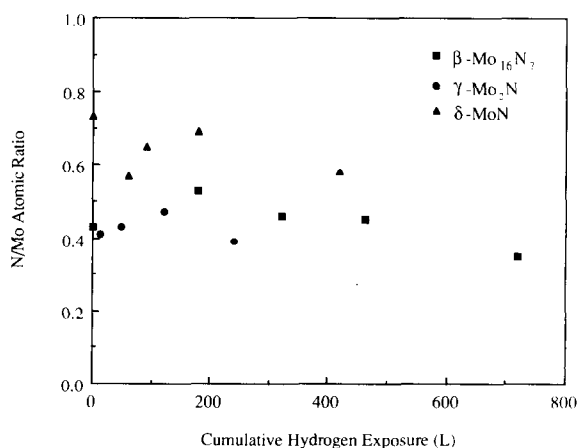

Fig. 11. The N/Mo atomic ratios for the β-$Mo_{16}N_7$, γ-Mo_2N and δ-MoN films following various H_2 exposures.

films possessed β_2 sites. We believe that the β_1 peak was due to a surface site while the β_2 peak was produced by desorption from a subsurface site. The peak temperature was constant with dose indicating that the β_1 state was due to a first-order process. In comparing the Mo nitride powders, which generally produced three H_2 desorption peaks, with the Mo nitride films we found that the low-temperature sites behaved in a similar fashion. Both the thin films and powders contained subsurface sites but with different energies. We observed that the δ-MoN film shared TPD features with the Mo nitride powder possessing the highest hydrodenitrogenation activity. This suggested that δ-MoN-like structures supported the highest activity sites. During the H_2 TPD experiments, nitrogen also desorbed from the Mo nitride surfaces. The amount of nitrogen that desorbed increased with increasing H_2 dose, suggesting a hydrogen-induced nitrogen desorption process. A large nitrogen desorption peak was observed at ~ 330 K and has been attributed to nitrogen bound to Mo atoms at the surface. Characteristics of the higher-temperature peaks were more complex. We suspect that the high-temperature nitrogen desorption peaks were influenced by hydrogen which diffused into the subsurface region.

Acknowledgments

References

[1] L. Volpe and M. Boudart, J. Solid State Chem. 59 (1985) 332.
[2] L. Volpe and M. Boudart, J. Solid State Chem. 59 (1985) 348.
[3] L. Volpe and M. Boudart, J. Phys. Chem. 90 (1986) 4874.
[4] S.T. Oyama, J.C. Schlatter, J.E. Metcalfe and J.M. Lambert, Jr., Ind. Eng. Chem. Res. 27 (1988) 1648.
[5] L. Leclercq, K. Imura, S. Yoshida, T. Barbee and M. Boudart, Preparation of Catalysts II, Ed. B. Delmon (Elsevier, New York, 1978) p. 627.
[6] R.B. Levy and M. Boudart, Science 181 (1973) 547.
[7] J.G. Choi, J.R. Brenner, C.W. Colling, B.G. Demczyk, J.L. Dunning and L.T. Thompson, Catal. Today 15 (1992) 201.
[8] C.W. Colling and L.T. Thompson, J. Catal. 146 (1994) 193.
[9] B.G. Demczyk, J.-G. Choi and L.T. Thompson, Appl. Surf. Sci. 78 (1994) 63.
[10] R. Bafrali and A.T. Bell, Surf. Sci. 278 (1992) 353.
[11] E.P. Donovan, U.K. Hubler, M. Mudholkar and L.T. Thompson, Nucl. Instr. Meth. Phys. Res., in press (1994).
[12] D. Briggs and M.P. Seah, Practical Surface Analysis by Auger and X-ray Photoelectron Spectroscopy (Wiley, New York, 1983).
[13] A.C. Liu and C.M. Friend, Rev. Sci. Instr. 57 (1986) 1519.
[14] M. Grunze, F. Bozso, G. Ertl and M. Weiss, Appl. Surf. Sci. 1 (1978) 241.
[15] M. Weiss, G. Ertl and F. Nitschké, Appl. Surf. Sci. 2 (1979) 614.
[16] P.A. Redhead, Vacuum 12 (1962) 203.
[17] P.W. Tamm and L.D. Schmidt, J. Chem. Phys. 51 (1969) 5352.
[18] F. Zaera, E.B. Kollin and J.L. Gland, Surf. Sci. 166 (1986) L149.
[19] H.R. Han and L.D. Schmidt, J. Phys. Chem. 75 (1971) 227.
[20] K.J. Leary, J.N. Michaels and A.M. Stacy, AIChE J. 34 (1988) 263.
[21] P.G. Shewmon, Diffusion in Solids (McGraw-Hill, New York, 1963).